Dilatancy and compaction effects on the submerged granular column collapse

Chun Wang, Yongqi Wang, Chong Peng, and Xiannan Meng

Citation: Physics of Fluids **29**, 103307 (2017); doi: 10.1063/1.4986502
View online: http://dx.doi.org/10.1063/1.4986502
View Table of Contents: http://aip.scitation.org/toc/phf/29/10
Published by the American Institute of Physics

Dilatancy and compaction effects on the submerged granular column collapse

Chun Wang,[1,a)] Yongqi Wang,[2,b)] Chong Peng,[3] and Xiannan Meng[2]
[1]*Collaborative Innovation Center for Advanced Ship and Deep-Sea Exploration, School of Naval Architecture, Ocean and Civil Engineering, Shanghai Jiao Tong University, 800 Dongchuan Road, 200240 Shanghai, People's Republic of China*
[2]*Chair of Fluid Dynamics, Department of Mechanical Engineering, Technische Universität Darmstadt, Otto-Berndt-Str. 2, 64287 Darmstadt, Germany*
[3]*Institute of Geotechnical Engineering (IGT), Universitaet fuer Bodenkultur, Feistmantelstrasse 4, 1180 Vienna, Austria*

(Received 19 May 2017; accepted 9 October 2017; published online 24 October 2017)

The effects of dilatancy on the collapse dynamics of granular materials in air or in a liquid are studied experimentally and numerically. Experiments show that dilatancy has a critical effect on the collapse of granular columns in the presence of an ambient fluid. Two regimes of the collapse, one being quick and the other being slow, are observed from the experiments and the underlying reasons are analyzed. A two-fluid smoothed particle hydrodynamics model, based on the granular-fluid mixture theory and the critical state theory, is employed to investigate the complex interactions between the solid particles and the ambient water. It is found that dilatancy, resulting in large effective stress and large frictional coefficient between solid particles, helps form the slow regime. Small permeability, representing large inter-phase drag force, also retards the collapse significantly. The proposed numerical model is capable of reproducing these effects qualitatively. *Published by AIP Publishing.* https://doi.org/10.1063/1.4986502

I. INTRODUCTION

Granular material collapse is a typical phenomenon for many natural and hazardous processes, such as debris flows,[1] landslides,[2] submarine avalanches[3]. Due to its damaging impacts to the safety of the structures or the geomorphology changing along the way it passes, granular material collapse has long been a research concern for geophysicists, hydrologists, and underwater engineers. There are a large amount of experimental and numerical studies dealing with the dry granular flows (such as sand and glass beads); among them, the so-called $\mu(I)$-rheology[4–6] has recently emerged as a major step towards consistently describing the dense granular flows.

Compared to the dry granular column collapse, however, the process of submerged granular column collapse has not yet been well understood, due to its complex interactions between fluids and solid particles. Recently, Rondon *et al.*[7] conducted an experimental study on the granular column collapse in an ambient fluid. Two regimes of the collapse, one being quick and the other being slow, are observed from the experiments, depending on the initial packing state, i.e., loose or dense, indicated by the initial volume fraction or equivalently the porosity. They employed a "pore pressure feedback" model to explain the formation of the different regimes. Granular materials are known to change volume when sheared: a dense packing dilates and a loose packing compacts. When the material is saturated with a fluid, the change in volume fraction induces a fluid motion and a pore pressure gradient, which can in turn affect the deformation of the material.[8–11] In the case of a dilatation, the liquid is sucked into the medium, pressing the grains together and enhancing the friction, whereas in the case of compaction, the liquid is expelled, decreasing the frictional interactions. This coupling between the dilatancy and the pore pressure is called "pore pressure feedback"[9,12] and has a dramatic influence on the way a landslide starts, as evidenced by the experiments carried out by Iverson[8] in the USGS large-scale facility. For a better understanding of the challenges and the recent developments on this topic, readers may refer to Refs. 7 and 13–16 and the references therein.

Although Rondon, Pouliquen, and Aussillous[7] have reported the experiments on granular column collapse in water/Ucon-oil mixture, the case of granular column collapse in water which is much less viscous than the former has not been reported. In this paper, experiments of granular column collapse are conducted to illustrate the different scenarios of granular flows in air, water, and glycerine aqueous solution. The novelties of this paper are as follows: Experimentally, the dilatancy behavior of granular materials immersed in fluids with different viscosities is investigated; numerically, a two-fluid Smoothed Particle Hydrodynamics (SPH) mixture model coupled with the critical state theory is developed to analyze the complex interactions between solid particles and the fluid. With the critical state theory, it is possible to investigate the effects of evolving dilatancy. Key factors influencing the formation of different regimes, namely, the dilatancy (or compaction) and the permeability (via hydraulic conductivity)

[a)]chunwang@sjtu.edu.cn
[b)]wang@fdy.tu-darmstadt.de

of the granular material, are investigated, which helps reveal the mechanisms of granular flows in the presence of an ambient fluid.

II. EXPERIMENTAL SETUP

The experiments investigate two-dimensional granular flows created by rapidly releasing particulate columns contained in a rectangular acrylic tank that is 50 cm long, 10 cm wide, and 15 cm high, as seen in Fig. 1. A column of granular material is delimited by a removable vertical wall which is maintained by two slots made on the side walls of the tank and can be removed rapidly to simulate a dam-break. Both dry and immersed granular column collapses are studied. In the immersed case, the tank is partially filled with a fluid. Two kinds of fluids, i.e., water (with dynamic viscosity $\mu = 1$ cP) and glycerine aqueous solution ($\mu = 12$ cP), are tested in the experiments to investigate the effects of permeability on the collapse. The particles used are glass beads of density $\rho_s = 2500$ kg/m^3 and mean diameter $d = 300$ μm, with a repose angle of $\theta = 25° \pm 0.4°$. The roughness of the tank walls is ignored because, irrespective of the roughness of the surface, a thin layer of grains is deposited on the bottom surface and the main flow takes place over these stationary grains.[17]

Dilatancy or compaction effects on the granular flow are the main concerns of the current study. Thus both loose and dense packing granular materials are prepared in the experimental procedure. The loose packing is made by gently pouring the glass beads into the reservoir delimited by the wall. The solid volume fraction ϕ_s in the loose state is found to be equal to $\phi_s = 0.57 \pm 0.004$ for the dry case and $\phi_s = 0.53 \pm 0.005$ for the immersed case. To create dense packing columns, we gently tap on the tank. By doing so, the solid volume fraction reached in our setup is 0.60 ± 0.003 for dry dense granular columns and 0.57 ± 0.003 for the immersed dense cases. Previous studies on tap induced compaction of granular matter suggest that the compaction process is homogeneous.[7]

Once the column is prepared at the desired mean volume fraction ϕ_i, the gate is suddenly removed by a heavy weight. Although a short time is needed to remove the gate from the tank, this period is so short (less than 0.1 s) that its influence on the collapse can be ignored. A side view using a video camera at 500 fps with a resolution of 1696×1710 pixels is employed to record the collapse processes. Each experimental case is repeated at least three times and a very high reproducibility is demonstrated.

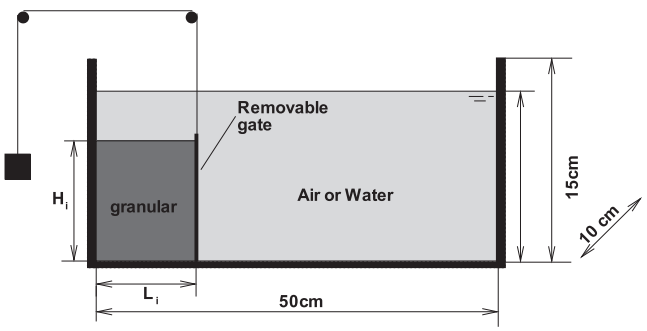

FIG. 1. Experimental setups for granular column collapse in air or in water.

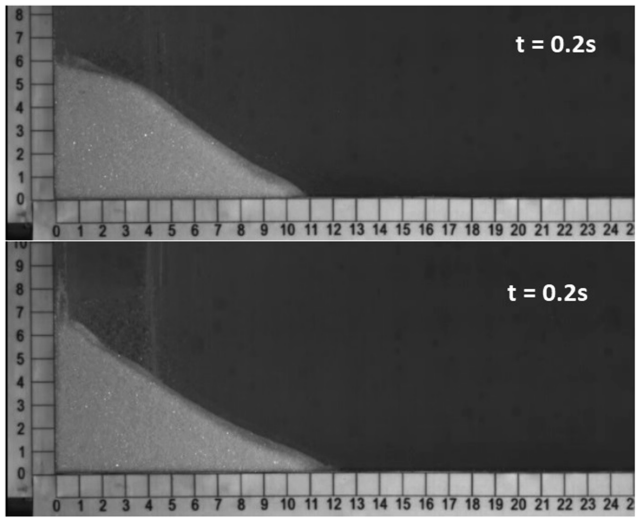

FIG. 2. Experimental observations of the overall profiles at a certain instant, in the case of dry granular column collapse. The grid interval of the ruler is 1 cm. Top: initially loose packing; bottom: initially dense packing. Multimedia view: https://doi.org/10.1063/1.4986502.1

III. EXPERIMENTAL OBSERVATIONS

Figure 2 (Multimedia view) shows the overall profiles at an instant during the collapse of dry granular columns, initially in loose and in dense packing, respectively. The evolution of the overall profiles during the collapse is shown in Fig. 3. Due to the compaction, the initial profile of the dense packing is shorter than that of the loose packing. It is seen that, for the loose packing, the upper part of the column drops quickly and the top becomes round at the very beginning. However, for the dense packing, the upper right corner falls first, thus the top is sharp at the beginning (the initial elevation of the upper right corner is caused by the disturbance of the removal of the gate). The final profiles for the two cases are almost the same, except that the runout distance in the loose case is a little further, which is caused by the quick fall of the upper part. In this experiment, the gate is removed faster in the dense case than in the loose case, which is why the initial front runout distances for the loose case are less than that for the dense case, as seen in Fig. 3. The collapse is over within 0.48 s for the loose packing and 0.52 s for the dense packing. Here the collapse is considered over when the difference of the profiles between consecutive 0.1 s is negligible.

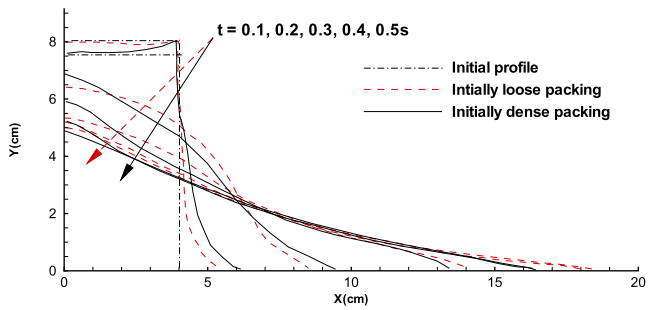

FIG. 3. Evolution of the overall profile in the case of dry granular column collapse. The time elapse between two consecutive profiles is 0.1 s.

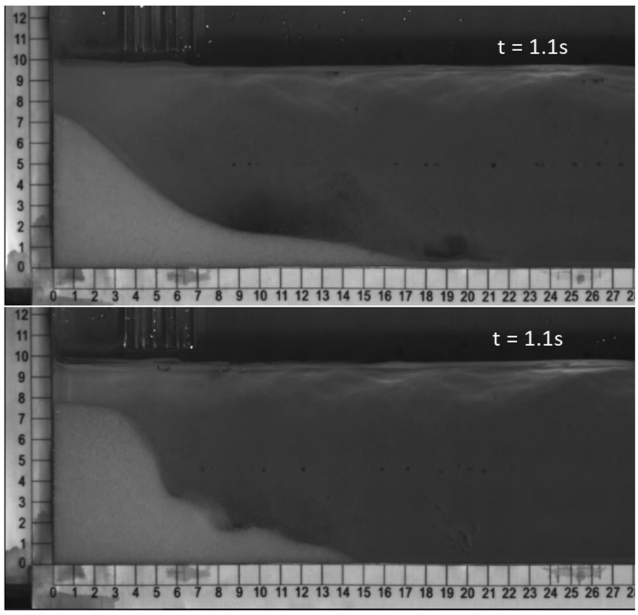

FIG. 4. Experimental observations of the overall profiles at a certain instant (t = 1.1 s), during the collapse of granular columns submerged in water. Top: initially loose packing; bottom: initially dense packing. Multimedia view: https://doi.org/10.1063/1.4986502.2

Figure 4 (Multimedia view) shows a snapshot from the experiments and demonstrates the collapse of granular columns immersed in water, respectively, for initially loose and dense packing. Evolutions of the granular profiles are shown in Figs. 5 and 6, respectively. In Fig. 5, the transient obtained for a low initial compactness is shown. Upon removal of the gate, as in the loose and dry cases, the upper part of the column drops quickly, resulting in a surge of the front. After that, the grains flow on the mild slope. The final profile is nearly a triangle. The interesting point is that the top has become blunt from the very beginning. This means that the summit of the pile starts to flow instantly. The large radius of the curvature of the top and the rapid decrease in height are both strong indications of a great depth of the flow in this loose case.

For a dense initial compactness, we observe a very different flow, displayed in Fig. 6. Upon removal of the gate, particles at the upper right corner and the right side fall off the pile almost freely, leading to a very steep profile with a round corner and small deposit at the toe of the column. When time goes on, the upper right corner fails and falls as a block,

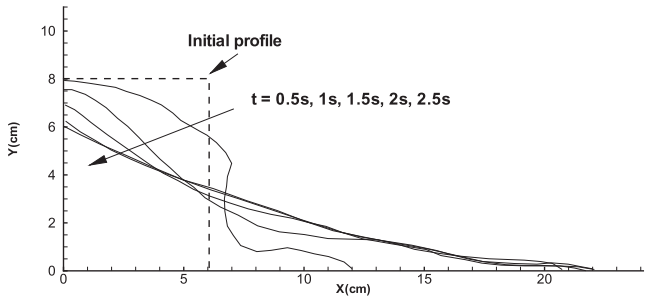

FIG. 5. Immersed loose granular column collapse in water. The time elapse between two consecutive profiles is 0.5 s.

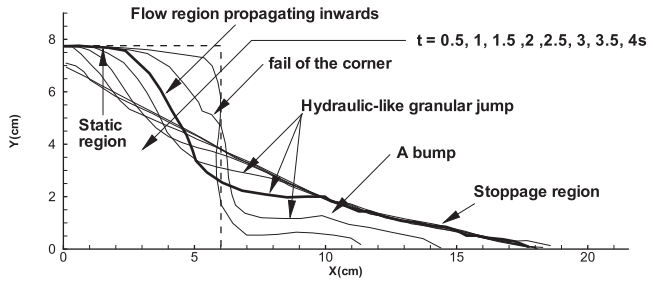

FIG. 6. Immersed dense granular column collapse in water. The time elapse between two consecutive profiles is 0.5 s.

resulting in a surge of the flow front and a bump when stopped. After that, particles move from the top of the column down a steep slope to a mild slope formed by the motionless particles which have previously fallen down. Thus, the granular profile at an instant (e.g., the bolded curve in Fig. 6) can be divided into three regions, i.e., the stoppage region of a small incline angle, the flow region of large angle (typically >40°) and inwards propagating, and the left static region which remains perfectly still until the flowing region reaches it. The abrupt change in the flow regime induces the formation of a "hydraulic-like granular jump," a thin and fast flowing layer being resisted by a thick and slow flowing layer.[18]

Compared to the dry case, the collapse in water lasts much longer. The collapse of the loose packing in water is over within 2.41 s, while for the dense packing, it takes 3.95 s.

Figure 7 (Multimedia view) shows the snapshot of granular column collapse in glycerine aqueous solution. Granular collapse in glycerine aqueous solution shows similar phenomena as that in water, i.e., the collapse of a loose packing is characterized by the mobilization of the whole column from the beginning, while the collapse of a dense packing begins from erosion of the surface, followed by one or two failures of the upper right corner. The main difference is that the collapse

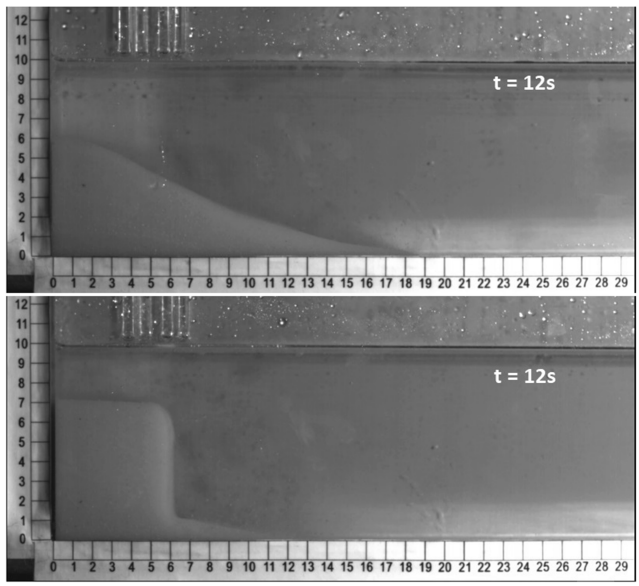

FIG. 7. Experimental observations of the overall profiles at a certain instant (t = 12 s), during the collapse of granular columns submerged in glycerine aqueous solution. Top: initially loose packing; bottom: initially dense packing. Multimedia view: https://doi.org/10.1063/1.4986502.3

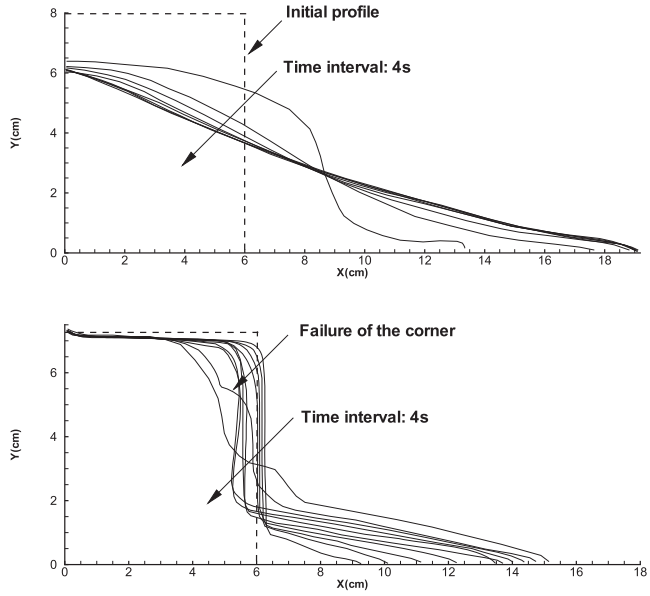

FIG. 8. Granular column collapse in glycerine aqueous solution. The time elapse between two consecutive profiles is 4 s. Top: initially loose packing; bottom: initially dense packing.

in a solution with a larger viscosity is much slower than in water, due to the weaker permeability and slow pore pressure dissipation of the former. In our experiments, the collapse for the loose packing in solution lasts tens of seconds and for the dense packing, minutes. The temporal evolution of the granular profile for this case is shown in Fig. 8. Our observation is in accordance with that of Rondon *et al.*[7]

These preliminary observations strongly suggest that the initial packing state is crucial to the study of the granular collapse in a fluid. Also the permeability plays a key role. In Sec. IV, we propose a theoretical model to reproduce the experimental observations.

IV. THEORETICAL BACKGROUND

The role of the ambient fluid can be investigated through a two-fluid continuum mixture theory.[13,19,20] In this two-fluid flow, the grains and the fluid are described as two continuum phases characterized by different velocities, different stresses, and interacting through hydrodynamics forces. The mass and momentum conservation laws can be formally derived from local averaging, the problem being the reasonable choice of the constitutive laws for each phase and the choice of the interacting forces between both phases. In the current study, the water is considered as a Newtonian fluid, and the constitutive relationship for it is well known. Here we only give a brief description on the constitutive relationship for the granular material and the interaction model between water and grains.

During the collapse process, the granular material undergoes plastic deformation, i.e., irreversible deformations occurring beyond the elastic regime. The two issues associated with plasticity are the following: what is the maximum stress level a granular medium can sustain before being irreversibly deformed and how does the deformation take place beyond the threshold? In this paper, the granular material is considered as an elastic-perfectly plastic material with a Drucker-Prager yield criterion

$$-\sqrt{J_2} = 3\alpha_\theta I_1 - k_c, \tag{1}$$

where I_1 is the first invariant of the total stress tensor of the granular matter, J_2 is the second invariant of the deviatoric stress tensor, α_θ and k_c are constants that can be related to the cohesion c and the friction angle θ of the Mohr-Coulomb failure criterion by matching the two models. In this paper, cohesion c is considered as zero, hence $k_c = 0$. For a plane strain problem, α_θ is determined by

$$\alpha_\theta = \frac{\tan\theta}{\sqrt{9 + 12\tan^2\theta}}. \tag{2}$$

If we consider I_1 as a measure of the mean solid pressure and J_2 as a measure of the shear stress, Eq. (1) is in fact a variation of Coulomb's friction law which depicts the internal friction between particles.

In computational plasticity theory, it is assumed that the total strain in a body can be decomposed into an elastic part and a plastic part. The elastic part of the strain can be computed from a linear elastic constitutive law, e.g., Hooke's law. To model the plastic part, however, we need a flow rule that states how the plastic deformation takes place once the stress threshold has been reached.

Granular materials are known to change volume when sheared: a dense packing dilates and a loose packing compacts. Thus the so-called non-associated flow rule is suitable for the granular flow, in which the plastic potential function $H(I_1,J_2)$ has the form

$$H(I_1, J_2) = \sqrt{J_2} + 3I_1 \sin\psi, \tag{3}$$

where ψ is the dilatancy angle. Dilatancy characterizes the volume change observed in granular materials subjected to shear deformation, as depicted in Fig. 9. A zero dilatancy angle indicates that the material is plastically incompressible. With the non-associated flow rule, the constitutive relationship for soil is

$$\begin{aligned}\dot{\tilde{\sigma}}_s^{\alpha\beta} - \tilde{\sigma}_s^{\alpha\gamma}\dot{\omega}_s^{\beta\gamma} - \tilde{\sigma}_s^{\gamma\beta}\dot{\omega}_s^{\alpha\gamma} &= 2G\dot{e}_s^{\alpha\beta} + K\dot{\varepsilon}_s^{\gamma\gamma}\delta^{\alpha\beta} \\ -\dot{\lambda}\left[9K\sin\psi\delta^{\alpha\beta} + G/\sqrt{J_2}\tilde{\tau}_s^{\alpha\beta}\right],\end{aligned} \tag{4}$$

where α and β are free indices and γ is a dummy index, with $\alpha,\beta,\gamma \in \{1,2,3\}$; $\delta^{\alpha\beta}$ is Kronecker's delta, $\delta^{\alpha\beta} = 1$ if $\alpha = \beta$ and $\delta^{\alpha\beta} = 0$ if $\alpha \neq \beta$; $\dot{\tilde{\sigma}}_s^{\alpha\beta}$ is the total stress rate tensor; $\tilde{\tau}_s^{\alpha\beta} = \tilde{\sigma}_s^{\alpha\beta} - \frac{1}{3}\tilde{\sigma}_s^{\gamma\gamma}\delta^{\alpha\beta}$ is the deviatoric part of the total stress tensor $\tilde{\sigma}_s^{\alpha\beta}$; $\dot{e}_s^{\alpha\beta}$ is the deviatoric part of the strain rate tensor $\dot{\varepsilon}_s^{\alpha\beta}$; G is the shear modulus and K is the bulk modulus.

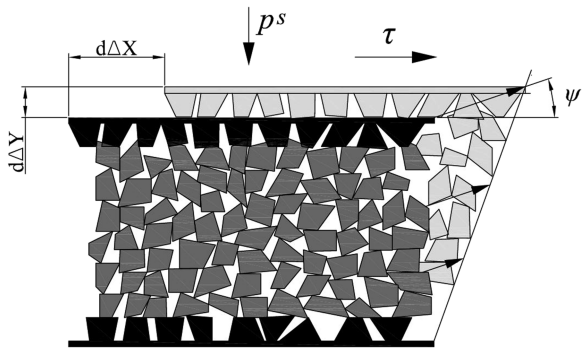

FIG. 9. The definition of the dilatancy angle ψ in a plane shear.

G and K are related to Young's modulus E and Poisson's ratio ν through

$$K = \frac{E}{3(1-2\nu)}, \quad G = \frac{E}{2(1+\nu)}. \tag{5}$$

In (4), $\dot{\lambda}$ is the rate of change of the so-called plastic multiplier λ dependent on the state of stress and load history and is given by

$$\dot{\lambda} = \frac{3\alpha_\theta K \dot{\varepsilon}_s^{\gamma\gamma} + (G/\sqrt{J_2})\tilde{\tau}_s^{\alpha\beta}\dot{\varepsilon}_s^{\alpha\beta}}{27\alpha_\theta K \sin\psi + G}. \tag{6}$$

Note that the left hand side of (4) has been replaced by the Jaumann rate, in which $\dot{\omega}_s^{\alpha\beta}$ is the rotational rate tensor

$$\dot{\omega}_s^{\alpha\beta} = \frac{1}{2}\left(\frac{\partial v_s^\alpha}{\partial x^\beta} - \frac{\partial v_s^\beta}{\partial x^\alpha}\right), \tag{7}$$

with $\boldsymbol{v}_s$ being the velocity of the solid particles.

In this paper, a critical state theory[21] is employed to determine the dilatancy angle ψ. According to this theory, the evolutions of the solid volume fraction and of the shear stress in a granular material subjected to plane-shear at a shear rate $\dot{\gamma}$ under a confining pressure p^s can be described by[22]

$$\frac{1}{\phi_s}\frac{\mathrm{d}\phi_s}{\mathrm{d}t} = -\tan\psi\ \dot{\gamma}, \tag{8}$$

$$\tau^s = \tan\psi\ p^s + \tau_{eq}, \tag{9}$$

$$\tan\psi = K_3(\phi_s - \phi_{eq}), \tag{10}$$

where τ_{eq} and ϕ_{eq} are the stress and the granular volume fraction obtained in the steady regime, respectively; K_3 is a constant to be calibrated. The first equation is a rewriting of the kinematic condition and stipulates how the volume fraction ϕ_s evolves with the strain γ and results from the definition of the dilatancy angle. In fact, from the mass conservation and the definitions of the dilatancy angle ψ and the strain γ, one can get Eq. (8).[23] The second equation means that the change in volume fraction implies an additional stress contribution due to the geometrical entanglement. The last equation is a closure relation, obtained by fitting the experimental measurements and assuming that the dilatancy angle is proportional to the difference between the actual volume fraction and the critical volume fraction corresponding to the steady state. Rewriting the second equation as $\tau^s = \tan(\theta+\psi)p^s$, we realize immediately the fact that the dilatancy angle ψ plays the role of adjusting the apparent friction angle θ: the dilation of a dense packing ($\psi > 0$) is accompanied by an increase of the apparent friction coefficient, the increase being equal to the dilatancy, whereas the compaction of a loose packing ($\psi < 0$) corresponds to a decrease of the apparent friction. Bearing this in mind, the coefficient α_θ in (1) should be replaced by

$$\alpha = \frac{\tan(\theta+\psi)}{\sqrt{9+12\tan^2(\theta+\psi)}}. \tag{11}$$

In Eq. (9), p^s is the normal stress acting on the granular skeleton. It is also called effective stress in soil mechanics. According to the principle of effective stress in soil mechanics, the total normal stress σ of the mixture can be expressed as the sum of pore pressure p and an effective normal stress p^s, as

$$\sigma = p^s + p, \tag{12}$$

which indicates that in the presence of constant σ, increasing in p will cause commensurate reduction in the effective normal stress p^s. Dilatancy changes the pore pressure, or equivalently the effective normal stress, as a consequence, also the frictional force between particles according to Coulomb's friction law. This phenomenon is called "pore pressure feedback"[1] and will be shown in our numerical simulation.

The interaction force $\boldsymbol{f}_\eta$ ($\eta = l,s$ for fluid and solid, respectively) is the force exerted on phase η by the other constituent. The interaction force $\boldsymbol{f}_s$ (i.e., $-\boldsymbol{f}_l$) is assumed to be in the form (see, e.g., Ref. 24)

$$\boldsymbol{f}_s = -\phi_s\nabla p + C_\mathrm{d}(\boldsymbol{v}_l - \boldsymbol{v}_s), \tag{13}$$

where ϕ_η is the volume fraction of phase η, satisfying $\phi_l + \phi_s = 1$ for a saturated liquid-solid mixture. Here the second term on the right-hand side is simply an inter-phase drag force, with C_d being the drag coefficient. The first term can be identified as a buoyancy force, e.g., the surface pressure exerted across the surface of the solids because of the surrounding fluid.

In this paper, the drag coefficient C_d in (13) can be derived from Darcy's law as

$$C_\mathrm{d} = \phi_l\gamma_w/k, \tag{14}$$

where k is called hydraulic conductivity with the dimensions of velocity [LT^{-1}], $\gamma_w = \rho_l g$ is the specific weight expressed with the partial density ρ_l of the water. $\rho_l = \phi_l\tilde{\rho}_l$ with $\tilde{\rho}_l$ being the true density of water. k is a constant depending not only on the type of the granular material but also on the type of the fluid (via dynamic viscosity μ) percolating through it. We find that hydraulic conductivity k plays an important role in the dynamics of the mixture flow. As we have observed from the experiments, in a solution with a low hydraulic conductivity, such as the glycerine aqueous solution, a granular column collapses very slowly. This is reasonable because, as we know, hydraulic conductivity depicts whether the fluid can flow through the porous media easily or not. Lower hydraulic conductivity indicates that the fluid can hardly percolate through the granules, leading to a slow collapse. Thus, it is very important to choose an appropriate hydraulic conductivity for the dense granular column collapse. In this paper, k is determined by the following Kozeny-Carman formula:[21]

$$k = K_p\tilde{\rho}_l g/\mu, K_p = \alpha d^2, \alpha = (1-\phi_s)^3/150\phi_s^2, \tag{15}$$

TABLE I. Material properties used in the computation for an initial 6 cm × 8 cm ($L_i \times H_i$) granular column collapse in fluids.

Property	Symbol	Value
True density of grains	$\tilde{\rho}_s$	2500 kg/m^3
Diameter of glass beads	d	300 μm
Young's modulus of grains	E	150 MPa
Poisson's ratio of grains	ν	0.3
Internal friction angle	θ	25°
Cohesion	k_c	0
Initial solid volume fraction	ϕ_i	0.55 (loose), 0.60 (dense)
Equilibrium volume fraction	ϕ_{eq}	0.58
Hydraulic conductivity	k	0.0005 m/s (in water), 0.000 05 m/s (in solution)
Viscosity of the fluids	μ	0.001 Pa s (in water), 0.012 Pa s (in solution)
Parameter in Eq. (10)	K_3	4.0

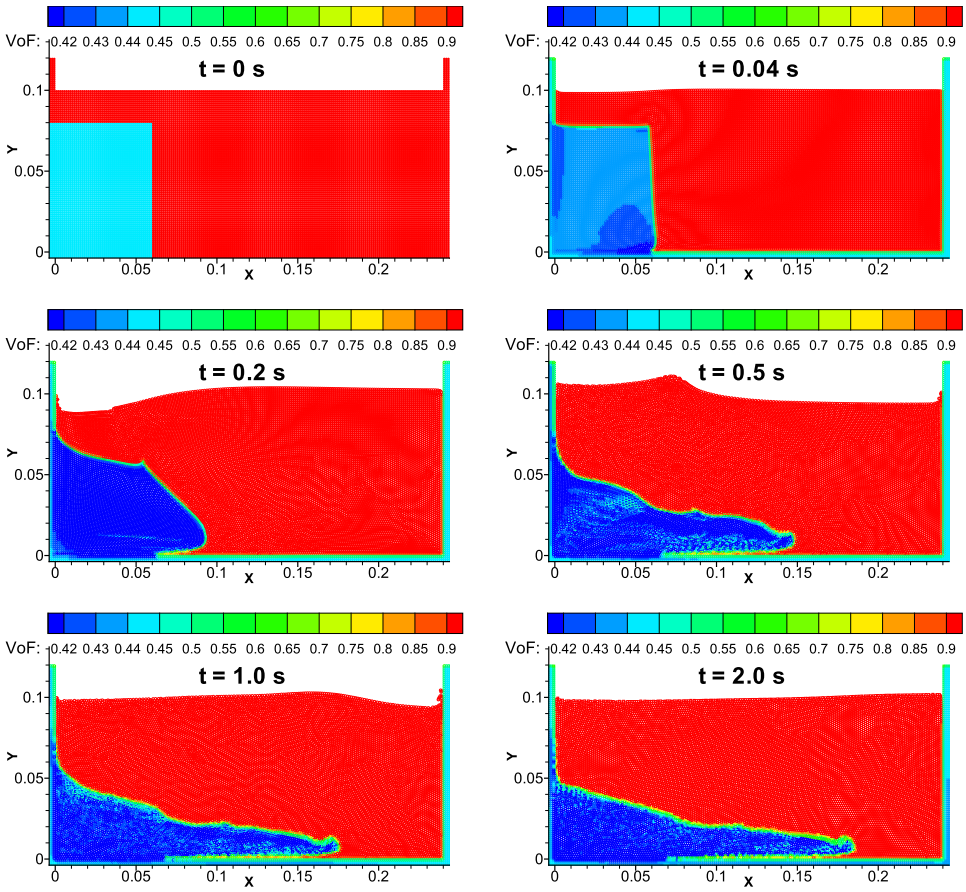

FIG. 10. Evolution of water volume fraction during the collapse of a loose pack.

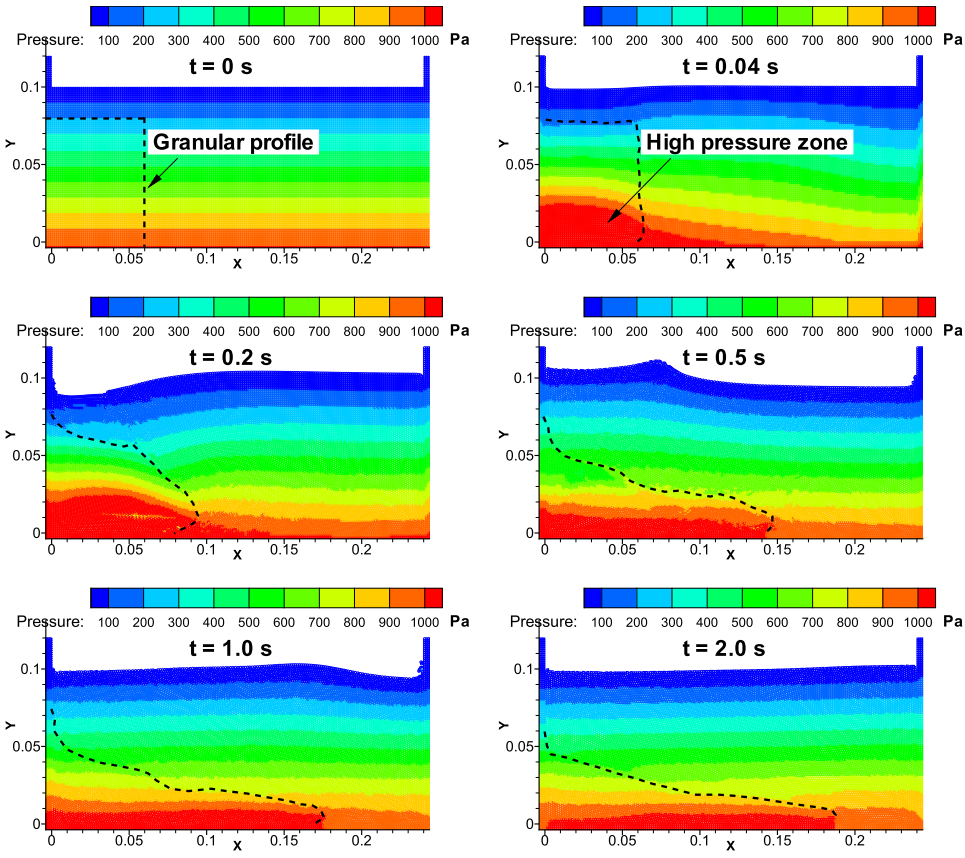

FIG. 11. Water pressure field during the collapse of a loose pack. The dashed line indicates the surface of the granular-fluid mixture.

where K_p is the permeability of the porous media formed by the particles and has the dimensions of a length squared.

V. NUMERICAL MODEL AND RESULTS

In the current study, the so-called weakly compressible SPH (WCSPH) method is employed to investigate the fluid dynamics. SPH is now a well-known numerical method, and we assume the reader is rather familiar with its basics. Thus, we will not describe the classical SPH interpolation and operators. For an extensive formulation of the two-fluid mixture SPH model, please see our recent paper[19] and the references therein.

Material properties used in the calculation are shown in Table I. In this table, Young's modulus E and Poisson's ratio ν are used to calculate G and K according to (5). For the problem of a granular column collapse studied here, the morphology of the deposit is not sensitive to E since the elastic deformation is negligibly small. A smaller E is employed here, in order to use larger time steps and make the computation stable. Hydraulic conductivity k is used to calculate the interphase drag force between water and solid particles according to (14). k takes the value of 0.0005 m/s and 0.000 05 m/s for water and glycerine aqueous solution, respectively, which are estimated using (15) for the packing of solid spheres of diameter $d = 300\ \mu$m. The equilibrium volume fraction ϕ_{eq} and the constant K_3 are introduced by the critical state theory and estimated according to Pailha and Pouliquen.[21]

There are a total of 15 360 fluid particles and 1824 solid particles generated regularly for water and solid phase in the tank, respectively. The initial particle spacing is 0.001 25 m. Computational time step size $\Delta t = 2.5 \times 10^{-6}$ s.

We consider first the case of granular column collapse in water. Figure 10 shows the volume fraction of water ϕ_l at some representative times during the collapse of an initially loose packing. According to the theory of the critical state, loose packing material exhibits compaction, i.e., the solid volume fraction will increase during the collapse process, leading to a decrease of the water volume fraction. Figure 10 confirms this trend. We can see that, upon release of the gate, the water volume fraction decreases rapidly and reaches its equilibrium value (i.e., 0.42 for water) in a short time. After that the volume fraction remains near the equilibrium position, as seen in Fig. 10.

Figure 11 shows the water pressure field at some representative times during the collapse of an initially loose packing. In our calculation, the pressure at the free surface is set to zero, and the pressure values at all other positions are relative to the free surface. As a result of the compaction, the interstitial pore water is squeezed out from the column, giving rise to a positive pore pressure field. Here, "positive" means the pressure is higher than the hydrostatic pressure of the surrounding fluid at the same depth. It can be seen that the particles come to rest in only a few seconds. Thus the collapse belongs to the quick regime.

The calculated profiles of the deposit at representative times are shown in Fig. 12 and compared with the experimental measurements. It is seen that, for the quick collapse regime, numerical results of SPH agree well with the experimental observations.

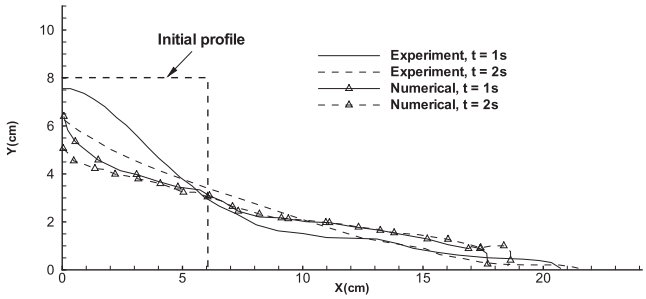

FIG. 12. Calculated profiles compared with experimental measurements for the case of a loose pack collapse in water.

Velocity vectors for water and solid particles are shown in Figs. 13 and 14. From Fig. 13, a large vortex at the upper right corner of the column can be seen at the initial stage of the collapse. During the later stage of the collapse, the vortex propagates and dissipates because of the viscosity of the fluid. For loose packing collapse, the flow layer of the solid particles is deep, thus a large part of the column is in moving, as seen in Fig. 14.

Now we come to the dense packing case. Figure 15 shows the water pressure field at some representative times during the collapse of a dense packing, while the temporal evolution of the water volume fraction is shown in Fig. 16. It can be seen that at the initial stage of the collapse, a low pressure

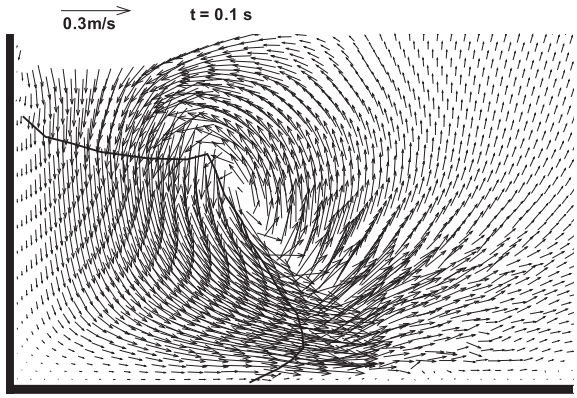

FIG. 13. Water velocity field at a certain instant (t = 0.1 s) during the collapse of an initially loose packing.

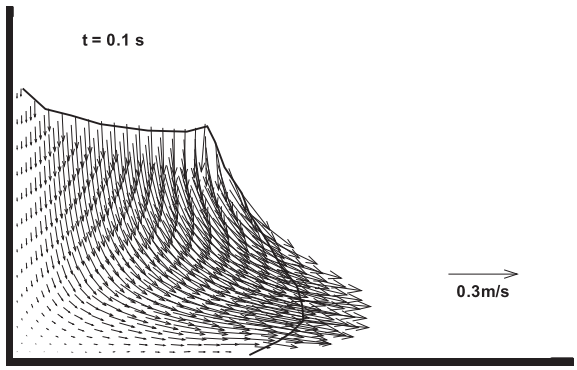

FIG. 14. Velocity field for solid particles at t = 0.1 s during the collapse of an initially loose packing immersed in water.

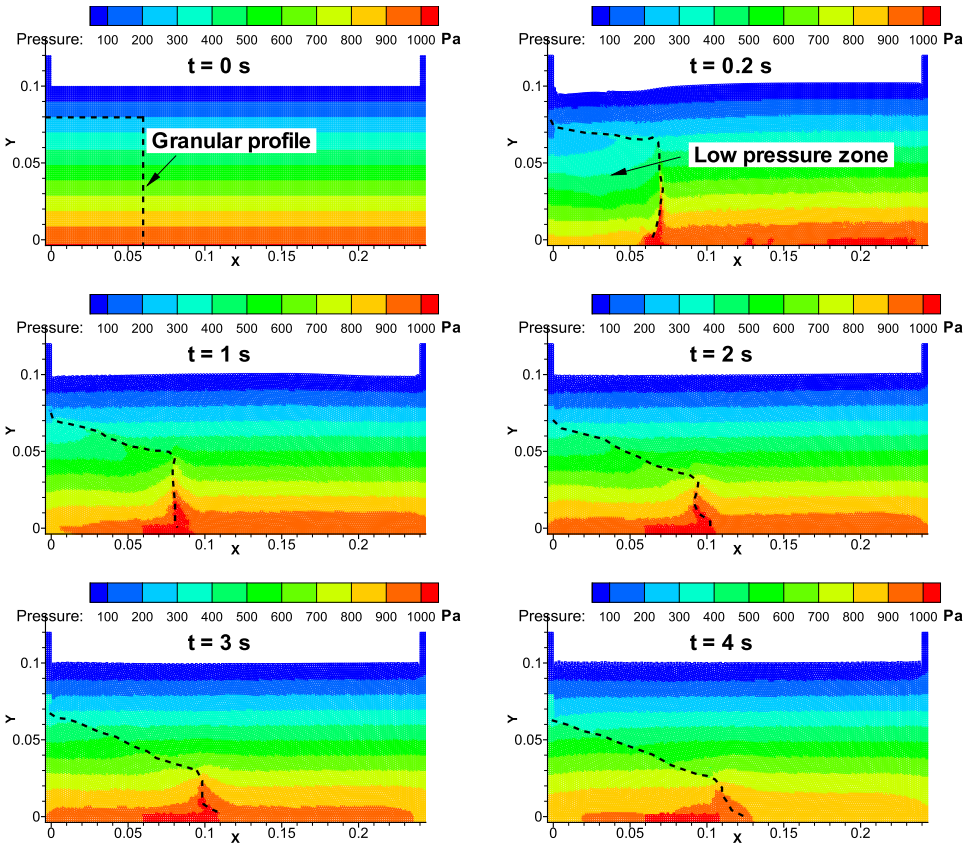

FIG. 15. Water pressure field during the collapse of a dense packing. The dashed line indicates the surface of the granular-fluid mixture.

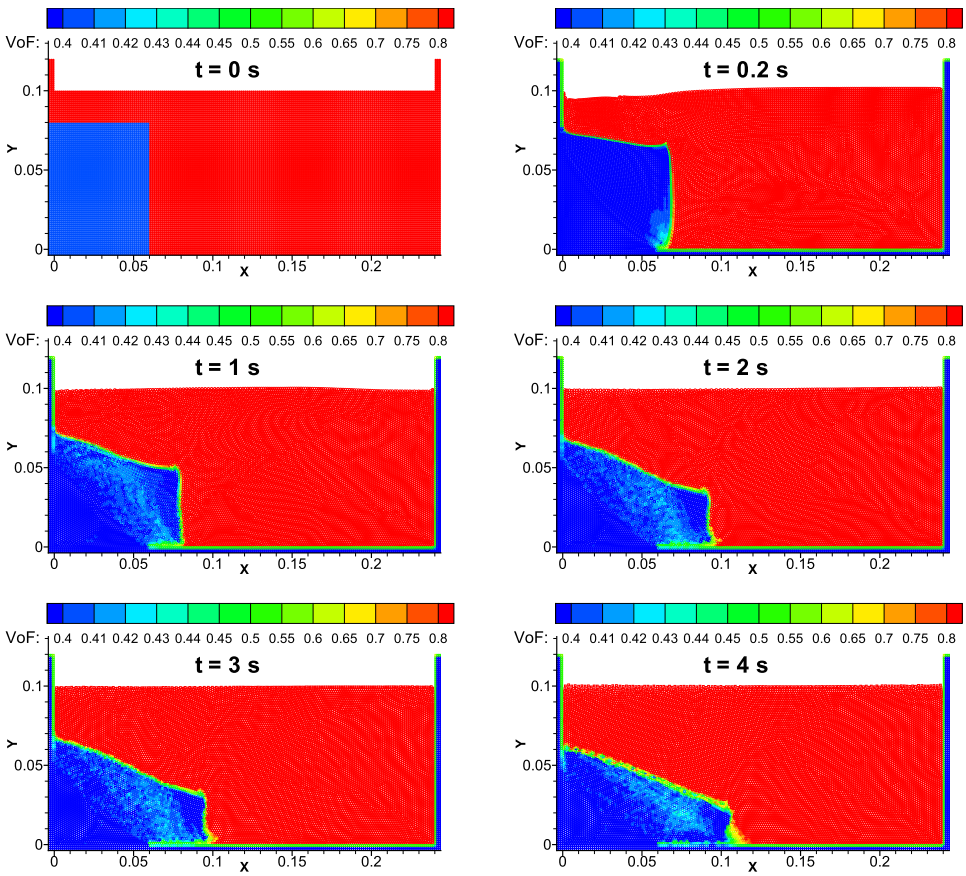

FIG. 16. Water volume fraction evolution during the collapse of a dense packing.

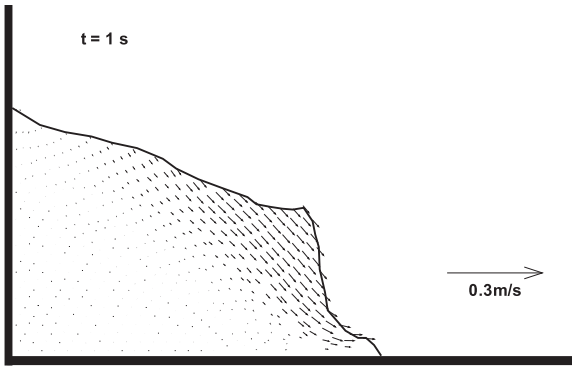

FIG. 17. Velocity field of solid particles during the collapse of a dense packing.

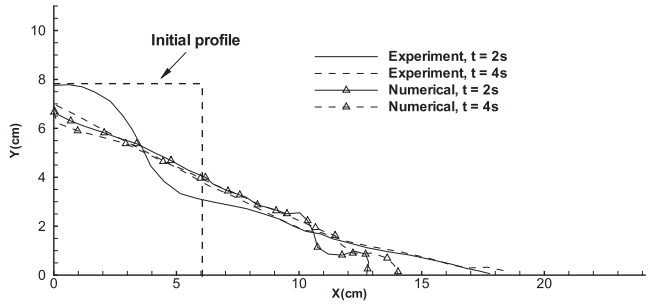

FIG. 18. Calculated profiles compared with experimental measurements for the case of a densely packing collapse in water.

zone is formed inside the granular column, due to the dilation occurrence when granular material is subjected to shearing. As a result, the interstitial pore volume is increased, as seen in Fig. 16, giving rise to a negative pore pressure and the fluid is drawn into the interstitial space. Here, again, "negative" means the pressure is lower than the hydrostatic counterpart of the surrounding fluid. As the fluid is sucked into the negative pore-pressure region, the negative pore-pressure subsides and the interstitial fluid pressure increases to restore that of the surrounding water during the collapse development. Compared to the loose case, the dense packing collapses much slowly, as shown also in the experimental data in Figs. 5 and 6.

Figure 17 shows the velocity vectors of solid particles for the case of dense packing collapse in water. In this case, the moving layer of the granular material is much shallower in comparison to that for an initially loose packing shown in Fig. 14. In other words, the main part of the column moves slowly, due to the dilatancy-enhanced friction.

We compare the calculated profiles of the deposit at representative times with the experimental measurements in Fig. 18 to investigate the validity of the proposed numerical model. It is seen that, for the slow collapse regime, numerical results of SPH agree well with the experimental observations. However, we have to point out that despite of the qualitative agreement between our numerical simulations and experimental observations, dense granular column collapse in fluids is still an open question for research. Our model is not able to reproduce some typical phenomena observed in the experiments. Among them, the occasional failure of the corner is a big challenge to numerical simulation. In fact, our theoretical model is a kind of "dilatant hardening" model in plasticity theory,[25] which is capable to model the "pore pressure feedback" mechanism. But, at the corner region, the pore pressure is quickly dissipated by the fast drainage there. Thus the corner is more easily to move. Dense granular material has another mechanism called "strain softening,"[26,27] which might also be accountable for the quick fall of the corner. However, this will be our future topic.

Application of the proposed numerical model for granular column collapse in glycerine aqueous solution is also performed. As an example, Fig. 19 illustrates the capability of the present SPH model in dealing with dense packing collapse in glycerine aqueous solution. It can be seen that the collapse of a dense packing column immersed in a sticky fluid is very slow, as observed from the experiments. Although much longer time computation can be performed, our numerical simulation shows that the collapse is only creeping. This can be explained by the dilatancy-enhanced friction and weak permeability of

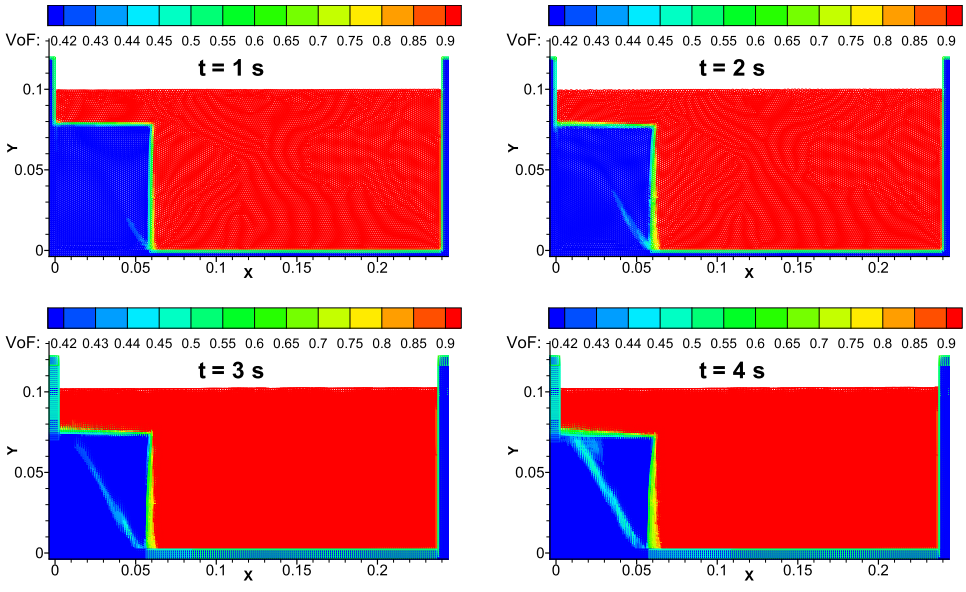

FIG. 19. Simulation of a densely packing column collapse in glycerine aqueous solution.

the fluid. Thus the ambient fluid has important influences on the morphology of the submerged granular column collapse. For all the cases, our numerical simulation recovers experimental observations with a good satisfaction.

VI. CONCLUSIONS

Dilatancy (or compaction) is well known for granular materials undergoing large deformations and has become an important research topic in recent years. Different regimes of the granular movements, i.e., quick or slow, have been previously observed in the experiments of immersed granular column collapse (see, e.g., Ref. 7). However, the complex interactions between solid particles and ambient fluids are still not well understood. The novelty of this paper lies in that we have conducted a series of experiments on granular column collapse with the presence of different ambient fluids, including air, water, and glycerine aqueous solution, to better understand the effects of viscosity on the dynamics of granular collapse in fluids. Both loose and dense packing are prepared in order to investigate the effects of dilatancy on the collapse. Compared with the dry case, granular column collapse in fluids shows quite different scenarios. First, two collapse regimes, one is quick and the other is slow, can be observed with the presence of the same fluid. This is explained by the dilation (compaction) behavior of dense (loose) packing through the enhancement (weakening) of the friction coefficient and "pore pressure feedback" mechanism. Second, the viscosity of the fluid also affects the collapse dynamics dramatically. In a sticky fluid, the collapse takes long time, due to the weak permeability of the fluid and the slow dissipation of the pore pressure.

Another novelty of this paper is that a two-fluid mixture smoothed particle hydrodynamics model, combined with the dilatancy effects and critical state theory, is proposed to reproduce the experimental observations. Agreement between our numerical results and the experimental observations illustrates the capability of the proposed numerical model in studying the complex interactions between fluid and solid particles in saturated mixture flows.

ACKNOWLEDGMENTS

This work is partly supported by the National Key Basic Research Program of China (Approval No. 2014CB046801).

[1]R. M. Iverson, "The physics of debris flows," Rev. Geophys. **35**, 245–296, doi:10.1029/97rg00426 (1997).
[2]F. Legros, "The mobility of long-runout landslides," Eng. Geol. **63**, 301–331 (2002).
[3]M. A. Hampton, H. J. Lee, and J. Locat, "Submarine landslides," Rev. Geophys. **34**, 33–59, doi:10.1029/95rg03287 (1996).
[4]P. Jop, Y. Forterre, and O. Pouliquen, "A constitutive law for dense granular flows," Nature **441**, 727–730 (2006).
[5]Y. Forterre and O. Pouliquen, "Flows of dense granular media," Annu. Rev. Fluid Mech. **40**, 1–24 (2008).
[6]I. R. Ionescu, A. Mangeney, F. Bouchut, and O. Roche, "Viscoplastic modeling of granular column collapse with pressure-dependent rheology," J. Non-Newtonian Fluid Mech. **219**, 1–18 (2015).
[7]L. Rondon, O. Pouliquen, and P. Aussillous, "Granular collapse in a fluid: Role of the initial volume fraction," Phys. Fluids **23**, 073301 (2011).
[8]R. M. Iverson, "Landslide triggering by rain infiltration," Water Resour. Res. **36**, 1897–1910, doi:10.1029/2000wr900090 (2000).
[9]R. M. Iverson, "Regulation of landslide motion by dilatancy and pore pressure feedback," J. Geophys. Res. **110**, f02015, doi:10.1029/2004jf000268 (2005).
[10]R. M. Iverson and D. L. George, "A depth-averaged debris-flow model that includes the effects of evolving dilatancy. I. Physical basis," Proc. R. Soc. A **470**, 20130819 (2014).
[11]D. L. George and R. M. Iverson, "A depth-averaged debris-flow model that includes the effects of evolving dilatancy. II. Numerical predictions and experimental tests," Proc. R. Soc. A **470**, 20130820 (2014).
[12]D. G. Schaeffer and R. M. Iverson, "Steady and intermittent slipping in a model of landslide motion regulated by pore-pressure feedback," SIAM J. Appl. Math. **69**, 769–786 (2008).
[13]C. Meruane, A. Tamburrino, and O. Roche, "On the role of the ambient fluid on gravitational granular flow dynamics," J. Fluid Mech. **648**, 381–404 (2010).
[14]C. Meruane, A. Tamburrino, and O. Roche, "Dynamics of dense granular flows of small-and-large-grain mixtures in an ambient fluid," Phys. Rev. E **86**, 026311 (2012).
[15]V. Topin, Y. Monerie, F. Perales, and F. Radjaï, "Collapse dynamics and runout of dense granular materials in a fluid," Phys. Rev. Lett. **109**, 188001 (2012).
[16]S. Savage, M. Babaei, and T. Dabros, "Modeling gravitational collapse of rectangular granular piles in air and water," Mech. Res. Commun. **56**, 1–10 (2014).
[17]G. Lube, H. E. Huppert, R. S. J. Sparks, and A. Freundt, "Collapses of two-dimensional granular columns," Phys. Rev. E **72**, 041301 (2005).
[18]T. Faug, P. Childs, E. Wyburn, and I. Einav, "Standing jumps in shallow granular flows down smooth inclines," Phys. Fluids **27**, 073304 (2015).
[19]C. Wang, Y. Wang, C. Peng, and X. Meng, "Smoothed particle hydrodynamics simulation of water-soil mixture flows," J. Hydraul. Eng. **142**, 04016032 (2016).
[20]C. Wang, Y. Wang, C. Peng, and X. Meng, "Two-fluid smoothed particle hydrodynamics simulation of submerged granular column collapse," Mech. Res. Commun. **79**, 15–23 (2017).
[21]M. Pailha and O. Pouliquen, "A two-phase flow description of the initiation of underwater granular avalanches," J. Fluid Mech. **633**, 115–135 (2009).
[22]M. Pailha, M. Nicolas, and O. Pouliquen, "Initiation of underwater granular avalanches: Influence of the initial volume fraction," Phys. Fluids **20**, 111701 (2008).
[23]B. Andreotti, Y. Forterre, and O. Pouliquen, *Granular Media: Between Fluid and Solid* (Cambridge University Press, 2013).
[24]X. Meng and Y. Wang, "Modelling and numerical simulation of two-phase debris flows," Acta Geotechnica **11**, 1027–1045 (2016).
[25]J. E. Andrade and R. I. Borja, "Modeling deformation banding in dense and loose fluid-saturated sands," Finite Elem. Anal. Des. **43**, 361–383 (2007), the Eighteenth Robert J. Melosh Competition.
[26]F. Zhang, B. Ye, and G. Ye, "Unified description of sand behavior," Front. Archit. Civ. Eng. China **5**, 121–150 (2011).
[27]E. J. Fern and K. Soga, "The role of constitutive models in MPM simulations of granular column collapses," Acta Geotechnica **11**, 659–678 (2016).